

Effects of alumina phases on CO₂ sorption and regeneration properties of potassium-based alumina sorbents

Soo Chool Lee · Min Sun Cho · Suk Yong Jung ·
Chong Kul Ryu · Jae Chang Kim

Received: 16 May 2013 / Accepted: 26 November 2013 / Published online: 4 December 2013
© Springer Science+Business Media New York 2013

Abstract A range of potassium-based alumina sorbents were fabricated by impregnation of alumina with K₂CO₃ to examine the effects of the structural and textural properties of alumina on the CO₂ sorption and regeneration properties. Alumina materials, which were used as supports, were prepared by calcining alumina at various temperatures (300, 600, 950, and 1,200 °C). The CO₂ sorption and regeneration properties of these sorbents were examined during multiple tests in a fixed-bed reactor in the presence of 1 vol% CO₂ and 9 vol% H₂O. The regeneration capacities of the potassium-based alumina sorbents increased with increasing calcination temperature of alumina. The formation of KHCO₃ increased with increasing calcination temperature during CO₂ sorption, whereas the formation of KAl(CO₃)(OH)₂, which is an inactive material, decreased. These results are due to the fact that the structure of alumina by the calcination temperature is related directly to the formation of the by-product [KAl(CO₃)(OH)₂]. The structure of alumina plays an important role in enhancing the regeneration capacity of the potassium-based alumina sorbent. Based on these results, a new potassium-based sorbent using δ -Al₂O₃ as a support was developed for post-combustion CO₂ capture. This sorbent maintained a high CO₂ capture capacity of 88 mg CO₂/g

sorbent after two cycles. In particular, it showed a faster sorption rate than the other potassium-based alumina sorbents examined.

Keywords Sorbent · Carbon dioxide · Alumina · Regeneration · Potassium carbonate

1 Introduction

Carbon dioxide (CO₂) is a major greenhouse gas that is released into the atmosphere by the combustion of fossil fuels (oil, natural gas, and coal) (IPCC 2005). CO₂ causes global warming, which may be disastrous to the environment. CO₂ can be removed from flue gases and waste gas streams using variety of methods, such as membrane separation, absorption with a solvent, and adsorption using molecular sieves (Hagewiesche et al. 1995; Mavroudi et al. 2003; Siriwardane et al. 2001; Takamura et al. 2001; Wilson et al. 2004).

The chemical sorption of CO₂ with regenerable solid sorbents containing alkali metal and alkali earth metal is one of the more efficient techniques for removing CO₂ (Abanades 2002; Arias et al. 2012; Chen et al. 2012; Gupta and Fan 2002; Hayashi et al. 1998; Hirano et al. 1995; Kwon et al. 2011; Lee et al. 2006; Li et al. 2010; Salvador et al. 2003; Zhang et al. 2011). The use of dry sorbents can be a cost-effective and energy efficient way of removing CO₂. In particular, alkali metal-based sorbents can be used for CO₂ capture at low temperatures (50–70 °C) with thermal regeneration occurring easily at temperatures <150 °C. Alkali metal carbonates, such as Na₂CO₃ and K₂CO₃, react with CO₂ and H₂O and transform to alkali metal hydrogen carbonates after CO₂ sorption according to the reaction, M₂CO₃ + CO₂ + H₂O \rightleftharpoons 2MHCO₃ (M = Na, K) (Liang et al. 2004; Seo

S. C. Lee · S. Y. Jung
Research Institute of Advanced Energy Technology, Kyungpook
National University, Daegu 702-701, Korea

M. S. Cho · J. C. Kim (✉)
Department of Chemical Engineering, Kyungpook National
University, Daegu 702-701, Korea
e-mail: kjchang@knu.ac.kr

C. K. Ryu
Korea Electric Power Research Institute, Daejeon 305-380, Korea

et al. 2007; Yi et al. 2007, 2008, Zhao et al. 2009a, 2012). Water vapor is always necessary for the formation of potassium hydrogen carbonate in all reactions as shown in the absorption mechanism. Several studies have examined the efficiency of the chemical sorption of CO_2 over K_2CO_3 supported on porous materials, such as activated carbon, TiO_2 , ZrO_2 , silica gel, and Al_2O_3 , using cyclic fixed-bed or fluidized-bed operations under moist conditions (Lee et al. 2008a, b, 2009, 2011; Shigemoto et al. 2006; Zhao et al. 2009b, c).

To manufacture alkali metal-based sorbents with high physical strength, inorganic materials, such as gamma-alumina ($\gamma\text{-Al}_2\text{O}_3$), are commonly used as solid sorbents. On the other hand, potassium-based sorbents using alumina as an additive or support has a disadvantage in that there is a decrease in the CO_2 capture capacity during multiple sorption and regeneration tests at temperatures between 60 and 200 °C (Lee et al. 2006, 2011, 2013; Lee and Kim 2007; Okunev et al. 2000, 2003). This has been attributed to the formation of new by-products, such as $\text{KAl}(\text{CO}_3)_2 \cdot 1.5\text{H}_2\text{O}$ or $\text{KAl}(\text{CO}_3)_2(\text{OH})_2$, during CO_2 sorption of a potassium-based sorbent using $\gamma\text{-Al}_2\text{O}_3$ even at temperatures below 60 °C. An ideal dry sorbent must have a high CO_2 capture capacity, high sorption rate, excellent regeneration property, and high attrition resistance to remove CO_2 from flue gases in a fluidized/transport-bed reactor (Lee et al. 2008a). A previous paper reported that $\alpha\text{-Al}_2\text{O}_3$ is one of the most useful materials for designing ideal potassium-based sorbent for post-combustion CO_2 capture (Lee et al. 2013). This potassium-based sorbent using commercial $\alpha\text{-Al}_2\text{O}_3$ as a support exhibited high CO_2 capture capacity as well as excellent regeneration properties. On the other hand, this sorbent exhibited a slow sorption rate despite the excellent regeneration properties when a potassium-based sorbent was prepared using $\alpha\text{-Al}_2\text{O}_3$ as a support material. Moreover, the effects of the structure and textural properties of alumina on the CO_2 capture and regeneration properties and the sorption rate are unclear.

One of the main aims of this study was to develop a new potassium alumina sorbent with a high CO_2 capture capacity, excellent regeneration properties, and rapid sorption rate for post-combustion CO_2 capture. In addition, the physical properties and mechanism of the potassium-based sorbents using a range of alumina materials before/after CO_2 absorption were examined by X-ray diffraction (XRD), temperature programmed desorption (TPD), inductive coupled plasma (ICP), and BET.

2 Experimental

2.1 Preparation of alumina used as a support

Commercial alumina (Al_2O_3 , Aldrich, 99.9 %) and alumina (Al_2O_3) prepared by a precipitation method were used

as support materials for the preparation of potassium-based alumina sorbents in this study. Al_2O_3 was prepared by a precipitation method using aluminum nitrate nonahydrate $\text{Al}(\text{NO}_3)_3 \cdot 9\text{H}_2\text{O}$, Aldrich, 99.9 %) and sodium hydroxide (NaOH , Aldrich). $\text{Al}(\text{NO}_3)_3 \cdot 9\text{H}_2\text{O}$ was added to D.I. water (de-ionized water) at a level of 0.5 mol. The solution was then adjusted with 1.5 mol of NaOH until it reached a pH of 10. The resulting precipitate was aged for 12 h in the solution at room temperature. The product was washed sufficiently with D.I. water and dried at 80 °C. The dried Al_2O_3 was calcined in a furnace in air for 4 h at 300, 600, 950 and 1,200 °C.

2.2 Preparation of sorbent

The potassium-based sorbents used in this study were prepared by the impregnation of alumina (Al_2O_3) with K_2CO_3 . A typical preparation procedure for the sorbent supported on Al_2O_3 was as follows (Lee et al. 2006, 2008b, 2009): 5.0 g of the support was added to an aqueous solution containing 2.15 g of anhydrous alkali metal carbonate (K_2CO_3 , Aldrich) in 25 ml of de-ionized water. The content was mixed with a magnetic stirrer for 24 h at room temperature. After stirring, the mixture was dried in a rotary evaporator at 60 °C. The dried samples were calcined in a furnace with a N_2 flow (100 ml/min) for 4 h at 500 °C, except when boehmite (AlOOH) was used as a support for the sorbent material, which was calcined at 300 °C. The temperature ramping rate was 3 °C/min. The sorbents are denoted as follows: $\text{KAl}(\text{B})\text{I}30$, $\text{KAl}(\text{G})\text{I}30$, $\text{KAl}(\text{G-A})\text{I}30$, $\text{KAl}(\text{D})\text{I}40$, $\text{KAl}(\text{A})\text{I}30$ and $\text{KAl}(\text{A-A})\text{I}30$ sorbents, where K represents K_2CO_3 , Al(B), Al(G), Al(D), Al(A), Al(G-A) and Al(A-A) represent $\gamma\text{-AlOOH}$, $\gamma\text{-Al}_2\text{O}_3$, $\delta\text{-Al}_2\text{O}_3$, and $\alpha\text{-Al}_2\text{O}_3$, $\gamma\text{-Al}_2\text{O}_3$ (Aldrich) and $\alpha\text{-Al}_2\text{O}_3$ (Aldrich), respectively, I denotes the impregnation method, and 30 or 40 represents the K_2CO_3 loading.

2.3 Apparatus and procedure

CO_2 absorption and regeneration processes were performed in a fixed-bed quartz reactor, with a diameter of 1 cm. The reactor was placed in an electric furnace under atmospheric pressure. Half of the sorbent (0.5 g) was packed into the reactor. All volumetric gas flows were measured under standard temperature and pressure (STP) conditions. The temperatures of the inlet and outlet lines of the reactor were maintained above 100 °C to prevent the condensation of water vapor before being injected into the reactor and G.C. column. A 1/8 in. stainless tube packed with Porapak Q was used as the column. When the CO_2 concentration of outlet gases reached the same level as that of the inlet gas (1 vol%) in the CO_2 absorption process, nitrogen was introduced for a sufficient time in multiple tests, to

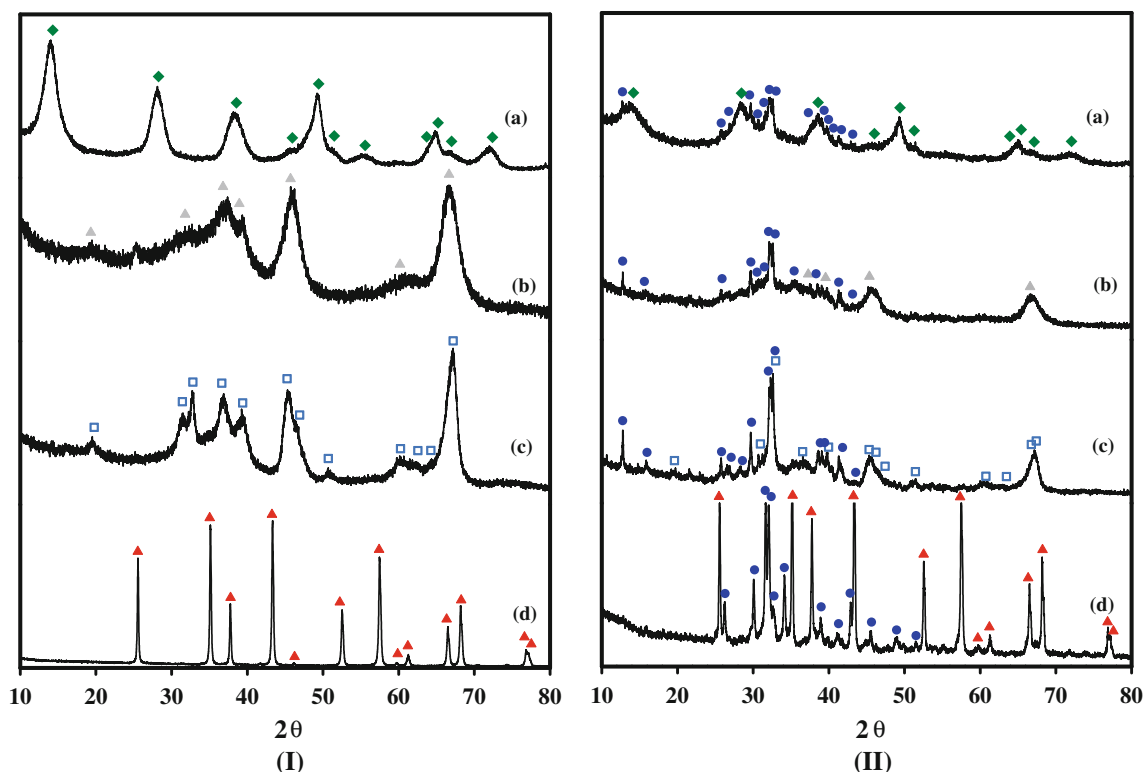


Fig. 1 XRD patterns of the **I** alumina materials calcined at 300, 600, 950 and 1,200 °C and the **II** fresh *a* KAl(B)I30, *b* KAl(G)I30, *c* KAl(D)I30, and *d* KAl(A)I30 sorbents before CO₂ sorption; filled

diamond γ -AlOOH; *grey triangle* γ -Al₂O₃; *square* δ -Al₂O₃, *filled triangle* α -Al₂O₃; *filled dot* K₂CO₃

regenerate the spent sorbents. The outlet gases from the reactor were analyzed automatically every 4 min using a thermal conductivity detector (TCD; Donam Systems Inc.) equipped with an auto sampler (Valco Instruments CO. Inc.).

X-ray diffraction (XRD; Philips, X'PERT) using Cu K α radiation was performed to identify the crystalline phases in the materials. The textural properties of the materials were measured from nitrogen adsorption–desorption at -196 °C by using a Micromeritics ASAP 2010 instrument. The amount of alkali metal impregnated was measured using an inductive coupled plasma-atomic emission spectroscopy (ICP-AES; Thermo, Thermo Jarrell Ash IRIS-AP). After dissolving K₂CO₃ dispersed on alumina with deionized water under stirring, the resulting solution was analyzed by ICP-AES.

3 Results and discussion

3.1 Structure identification of aluminas and sorbents

The structural changes in the alumina materials after calcination at various temperatures such as 300, 600, 950, and 1,200 °C, which were selected through a separate TG/DTA

test of boehmite, were examined by XRD (Fig. 1I). As expected, the XRD patterns of the alumina materials calcined at 300, 600, 950 and 1,200 °C showed a γ -AlOOH phase (JCPDS No. 49-0133), γ -Al₂O₃ phase (JCPDS No. 10-0425), δ -Al₂O₃ phase (JCPDS No. 46-1131), and α -Al₂O₃ phase (JCPDS No. 88-0826), respectively. The structural properties of the fresh KAl(B)I30, KAl(G)I30, KAl(D)I30, and KAl(A)I30 sorbents before CO₂ sorption were examined by XRD (Fig. 1II). The XRD pattern of the fresh potassium-based alumina sorbents showed only a separate K₂CO₃ phase (JCPDS No. 71-1466) in addition to each alumina phase without K–Al alloy products.

3.2 CO₂ capture and regeneration capacities of the potassium-based alumina sorbents

Figure 2 shows the breakthrough curves of the KAl(B)I30, KAl(G)I30, KAl(G-A)I30, KAl(D)I30, KAl(A)I30, and KAl(A-A)I30 sorbents at 1 and 5 cycles. The KAl(B)I30, KAl(G)I30, KAl(G-A)I30, KAl(D)I30, KAl(A)I30, and KAl(A-A)I30 sorbents were prepared by the impregnation of γ -AlOOH, γ -Al₂O₃, γ -Al₂O₃ (Aldrich), δ -Al₂O₃, α -Al₂O₃, and α -Al₂O₃ (Aldrich), respectively, with 30 wt% K₂CO₃. In the cases of the KAl(B)I30, KAl(G)I30, KAl(G-A)I30 and KAl(D)I30 sorbents, the breakthrough times were

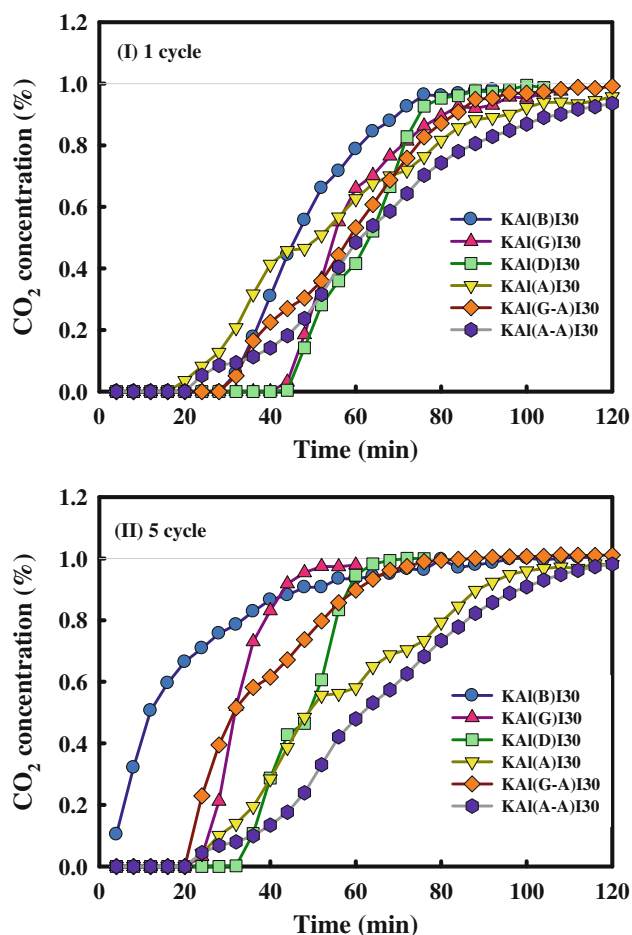


Fig. 2 Breakthrough curves of the potassium-based alumina sorbents such as KAl(B)I30, KAl(G)I30, KAl(G-A)I30, KAl(D)I30, KAl(A)I30 and KAl(A-A)I30 at **I** 1 and **II** 5 cycles

approximately 28, 40, 32, and 44 min, respectively. On the other hand, the breakthrough times of the KAl(A)I30 sorbents were approximately 16 min despite the excellent regeneration properties and were similar to the KAl(A-A)I30 sorbent using α -Al₂O₃ (Aldrich) as reported elsewhere (Lee et al. 2013). After 5 cycles, the breakthrough times of the KAl(B)I30, KAl(G)I30, KAl(G-A)I30, KAl(D)I30, KAl(A)I30, and KAl(A-A)I30 sorbents were 0, 20, 20, 32, 20, and 16 min, respectively.

Figure 3 shows the CO₂ capture capacities of the KAl(B)I30, KAl(G)I30, KAl(G-A)I30, KAl(D)I30, KAl(A)I30, and KAl(A-A)I30 sorbents during the multiple tests for sorption (60 °C) and regeneration (200 °C). The CO₂ capture capacities of the sorbent were calculated from the breakthrough curve during multiple tests. The theoretical value of the sorbent was calculated from moles of K₂CO₃ involved in the sorbent, when one mole of K₂CO₃ absorbed a stoichiometric amount of one mole of CO₂. The CO₂ capture capacities of the KAl(B)I30, KAl(G)I30, KAl(G-A)I30, and KAl(D)I30 sorbents decreased at 2 cycles. On the other hand,

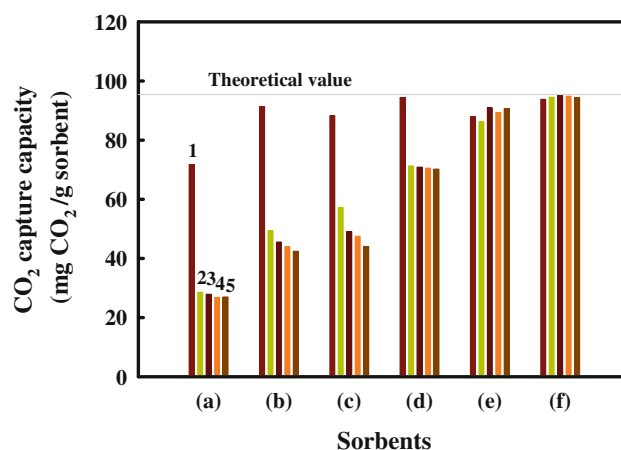


Fig. 3 CO₂ capture capacities of the potassium-based alumina sorbents during multiple tests for sorption (60 °C) and regeneration (200 °C) in the presence of 1 vol% CO₂ and 9 vol% H₂O; a KAl(B)I30; b KAl(G)I30; c KAl(G-A)I30; d KAl(D)I30; e KAl(A)I30; f KAl(A-A)I30

the KAl(A)I30 sorbent showed CO₂ capture capacities of approximately 90–95 mg CO₂/g sorbent and no deactivation during multiple cycles even at a regeneration temperature of 200 °C, similar to the result of the KAl(A-A)I30 sorbent reported in a previous paper (Lee et al. 2013). In addition to the CO₂ sorption and regeneration properties of the potassium-based sorbent, the sorption rate is an important factor. The CO₂ sorption rate of the KAl(A)I30 sorbent cannot be enhanced using α -Al₂O₃ as a support, which was prepared by precipitation, even though it can be regenerated completely at 200 °C. Nevertheless, the KAl(D)I30 sorbent had the longest breakthrough time and a high slope after the breakthrough point, but it decreased slightly during multiple tests. Considering that the sorption rate and regeneration properties are important factors in CO₂ capture, the KAl(D)I30 sorbent has potential for CO₂ capture in the low temperature range.

3.3 Effects of the structure and textural properties on the regeneration properties of potassium-based alumina sorbents

The C₅/C₁ ratio was calculated from Fig. 4 to identify the regeneration properties of the sorbents in detail. C₁ and C₅ represent the CO₂ capture capacity at 1 and 5 cycles, respectively. This value indicates the regeneration capacity of the sorbent. As shown in Fig. 4, the regeneration capacities of the KAl(B)I30, KAl(G)I30, KAl(D)I30 and KAl(A)I30 sorbents were 37.6, 46.5, 74.3 and 103.1 %, respectively, suggesting that the regeneration capacity increased with increasing calcination temperature of alumina used as a support. The deactivation problem of the alkali-based alumina sorbent using alumina could be solved using α -Al₂O₃ as a support. The KAl(A)I30 sorbent

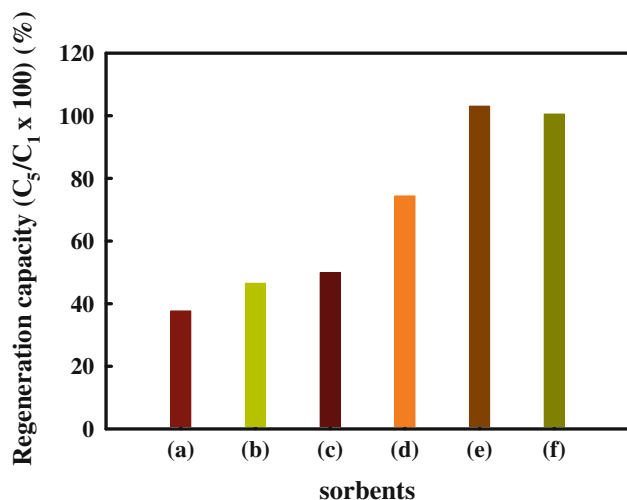


Fig. 4 Regeneration capacities ($C_5/C_1 \times 100$) of the potassium-based alumina sorbents such as *a* KAl(B)I30, *b* KAl(G)I30, *c* KAl(G-A)I30, *d* KAl(D)I30, *e* KAl(A)I30 and *f* KAl(A-A)I30

using α -Al₂O₃ as a support showed a similar result to that of the KAl(A-A)I30 sorbent, which was prepared using commercial α -Al₂O₃ (Aldrich), as reported in a previous paper (Lee et al. 2013). In particular, Fig. 4 shows that the regeneration capacity of the alkali-based alumina sorbent can be improved using δ -Al₂O₃ as a support. From these results, it was thought that the improved regeneration properties of the alkali-based alumina sorbent were attributed to the structural properties of the alumina support.

Table 1 lists the crystallite sizes of the alumina and the textural properties of alumina and the potassium-based alumina sorbents. The surface area of alumina decreased with increasing calcination temperature, whereas the average pore size increased, due to an increase in crystallite size, as shown in Table 1. It is well known that the surface area and average pore diameter are directly correlated with the crystallite size as reported by other researchers (Kim et al. 2007; Stichert and Schuth 1998). The regeneration capacity increased with decreasing surface area of alumina, suggesting that the enhanced regeneration capacity of the

sorbent was affected by the textural properties of alumina. On the other hand, although the surface areas of γ -Al₂O₃ and α -Al₂O₃ were higher than those of the commercial γ -Al₂O₃ and α -Al₂O₃ (Aldrich), respectively, the regeneration capacity of the KAl(G)I30 and KAl(A)I30 sorbents were similar to those of the KAl(G-A)I30 and KAl(A-A)I30 sorbents. In addition, although the surface area of δ -Al₂O₃ was similar to γ -Al₂O₃ (Aldrich), the regeneration capacity of the KAl(D)I30 sorbent was much higher than that of the KAl(G-A)I30 sorbent. Therefore, the improved regeneration properties of the potassium-based alumina sorbent can be explained by the structural properties of alumina rather than by the effect of the textural properties of alumina.

3.4 Structure identification of the sorbents after CO₂ sorption and regeneration

The structure changes in the KAl(B)I30, KAl(G)I30, KAl(D)I30 and KAl(A)I30, sorbents after CO₂ sorption and regeneration at 60 and 200 °C, respectively, were examined by XRD (Fig. 5). After CO₂ sorption, the XRD patterns of the KAl(B)I30, KAl(G)I30 and KAl(D)I30 sorbents showed KAl(CO₃)(OH)₂ phases (JCPDS No. 22-0791) and KHCO₃ phases (JCPDS No. 70-0995) (Lee et al. 2006, 2011, 2013; Lee and Kim 2007) as shown in Fig. 5I). In the case of the KAl(D)I30 sorbent, the intensity of the XRD peaks associated with the KHCO₃ phase was higher than those of the other sorbents. On the other hand, the XRD patterns of the KAl(A)I30 sorbents after CO₂ sorption showed a KHCO₃ phase in addition to an α -Al₂O₃ phase as shown in Fig. 5 (I-d), indicating that the XRD patterns are similar to that of the KAl(A-A)I30 sorbent as reported elsewhere (Lee et al. 2013). After regeneration under nitrogen at 200 °C, the XRD patterns of the KAl(B)I30, KAl(G)I30 and KAl(D)I30 sorbents revealed K₂CO₃ and KAl(CO₃)₂(OH)₂ phases. This means that KAl(CO₃)₂(OH)₂ is not converted to the original active material, such as K₂CO₃. These results suggest that the new by-product like KAl(CO₃)(OH)₂ is affected by the structure of alumina and that the regeneration capacity of the

Table 1 Crystallite sizes and textural properties of the alumina and potassium-based alumina sorbents

Sample name	Crystallite size (nm)	Surface area (m ² /g)	Pore volume (cm ³ /g)	Pore size (nm)	Sample name	Surface area (m ² /g)	Pore volume (cm ³ /g)	Pore size (nm)
γ -AlOOH	4.7	230.0	0.28	4.9	KAl(B)I30	8.4	0.04	18.2
γ -Al ₂ O ₃	4.4	183.5	0.35	7.6	KAl(G)I30	57.7	0.17	11.6
γ -Al ₂ O ₃ (Aldrich)	8.9	156.9	0.23	5.9	KAl(G-A)I30	27.7	0.07	9.7
δ -Al ₂ O ₃	6.2	158.5	0.52	13.3	KAl(D)I30	31.7	0.13	15.8
α -Al ₂ O ₃	45.3	15.5	0.24	62.9	KAl(A)I30	6.8	0.04	24.3
α -Al ₂ O ₃ (Aldrich)	103.4	0.1	0.0003	78.5	KAl(A-A)I30	0.1	0.0026	60.4

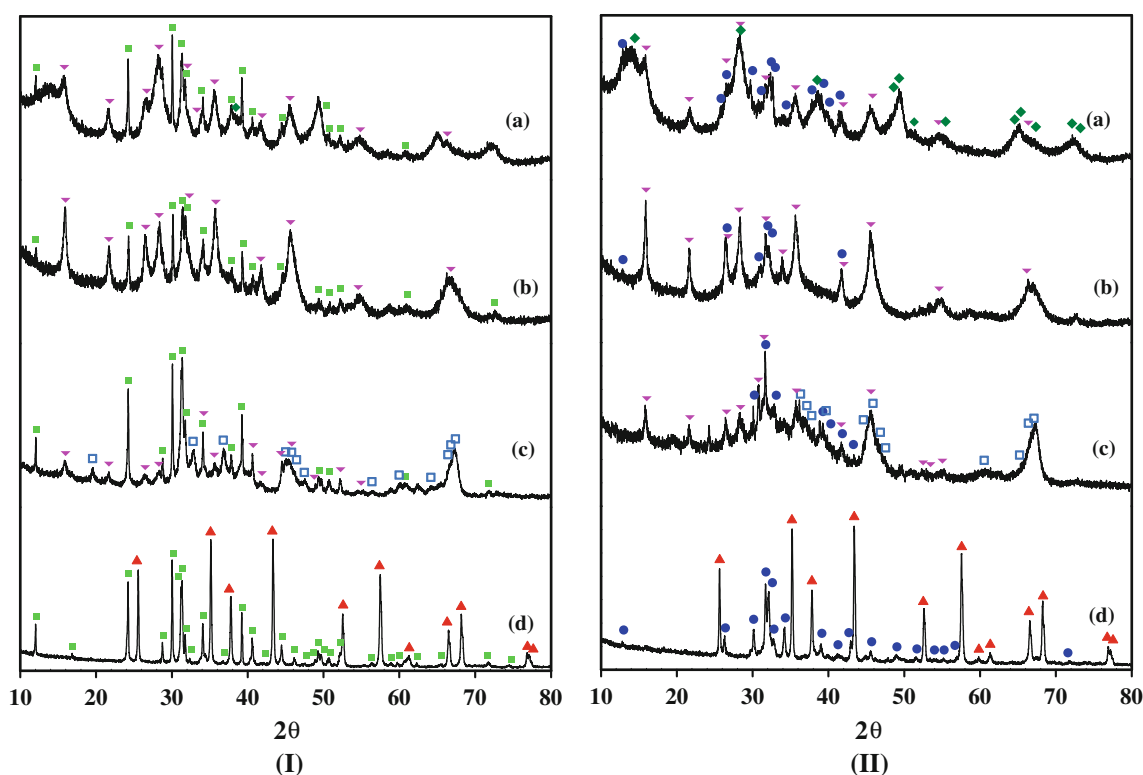


Fig. 5 XRD patterns of the *a* KAl(B)I30, *b* KAl(G)I30, *c* KAl(D)I30 and *d* KAl(A)I30 sorbents after **I** CO₂ sorption and **II** regeneration; (filled square) KHCO₃; (inverted triangle) KAl(CO₃)₂(OH)₂; (filled diamond) γ-AlOOH; (square) δ-Al₂O₃; (filled triangle) α-Al₂O₃; (filled dot) K₂CO₃

potassium-based alumina sorbent is related directly to the new by-product.

To confirm these results in detail, the TPD tests of these sorbents were carried out by measuring the concentration of CO₂ desorbed when the temperature ramping rate was 1 °C/min, as shown in Fig. 6I. The TPD results for the potassium-based alumina sorbents, such as KAl(B)I30, KAl(G)I30, KAl(D)I30 and KAl(A)I30, showed two CO₂ peaks. This suggests that there are two types of structures, due to the CO₂ desorption of KHCO₃ and KAl(CO₃)(OH)₂, as reported elsewhere (Lee et al. 2006, 2011, 2013; Lee and Kim 2007). Figure 6b shows the CO₂ desorption capacity calculated from each TPD peak area. As shown in Fig. 6II, the peak area of (A) for the KHCO₃ increased with increasing calcination temperature, whereas the peak area of (B) for the KAl(CO₃)(OH)₂ decreased. The structure of alumina by the calcination temperature is related directly to the formation of the by-product [KAl(CO₃)(OH)₂], which is an inactive material. The structure of alumina plays an important role in enhancing the regeneration capacity of the potassium-based alumina sorbent.

3.5 Development of new potassium-based δ-alumina sorbent

As mentioned previously, the KAl(D)I30 sorbent showed an excellent sorption rate compared to the other potassium-

based alumina sorbents examined, even though the sorbent showed deactivation during multiple tests due to the formation of a by-product. Considering that the CO₂ capture capacity of the KAl(D)I30 sorbent was maintained after two cycles, as shown in Fig. 2, it is believed that its CO₂ capture capacity can be increased by increasing the K₂CO₃ loading. The KAl(D)I40 sorbent was prepared by the impregnation of δ-Al₂O₃, which has a higher surface area (158.5 m²/g) and pore volume (0.52 cm³/g) than α-Al₂O₃, with 40 wt% K₂CO₃. The CO₂ capture capacity of the KAl(D)I40 sorbent was compared with those of the KAl(G)I40 and KAl(A)I40 sorbents using γ-Al₂O₃ and α-Al₂O₃. Figure 7 shows the CO₂ capture capacities of the KAl(G)I40, KAl(D)I40 and KAl(A)I40 sorbents during multiple tests. The KAl(G)I40 and KAl(D)I40 sorbents showed similar types of deactivation for KAl(G)I30 and KAl(D)I30 sorbents with 30 wt% K₂CO₃ during multiple tests. The KAl(A)I40 sorbent maintained a CO₂ capture capacity of approximately 94 mg CO₂/g sorbent during multiple cycles. When the amount of CO₂ sorption per 1 g of K₂CO₃ was calculated from this value, the KAl(A)I40 sorbent showed a CO₂ capture capacity of approximately 235 mg CO₂/g K₂CO₃. This was approximately 73 % of the theoretical value of the sorbent (318.3 mg CO₂/g K₂CO₃), which was calculated from the 40 wt% K₂CO₃ added to the sorbent. Considering that the CO₂ capture

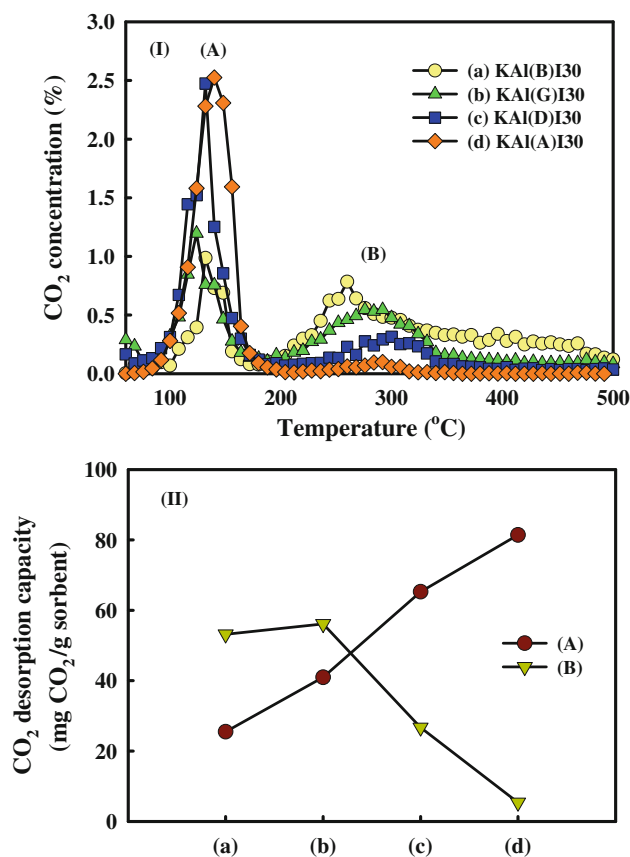


Fig. 6 **I** TPD results of the *a* KAl(B)I30, *b* KAl(G)I30, *c* KAl(D)I30 and *d* KAl(A)I30 sorbents after CO₂ sorption and **II** CO₂ desorption capacities calculated from each TPD peak area: A peak area in the temperature range 100–200 °C; B peak area in the temperature range 200–400 °C

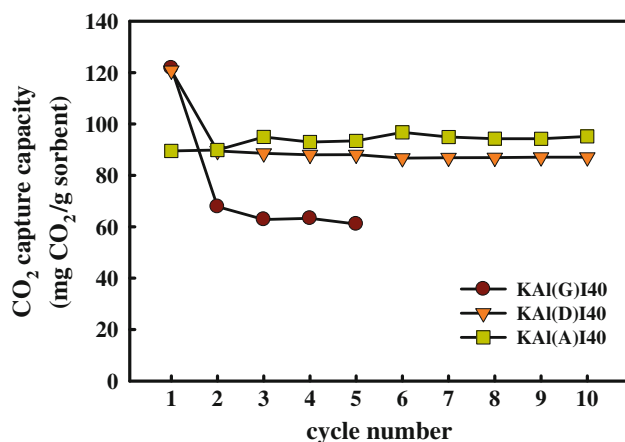


Fig. 7 CO₂ capture capacities of the KAl(G)I40, KAl(D)I40 and KAl(A)I40 sorbents during the multiple tests

capacity of the KAl(A)I30 sorbent is 292 mg CO₂/g K₂CO₃, which is 92 % of the theoretical capacity of the sorbent with 30 wt% K₂CO₃, the amount of CO₂ sorption

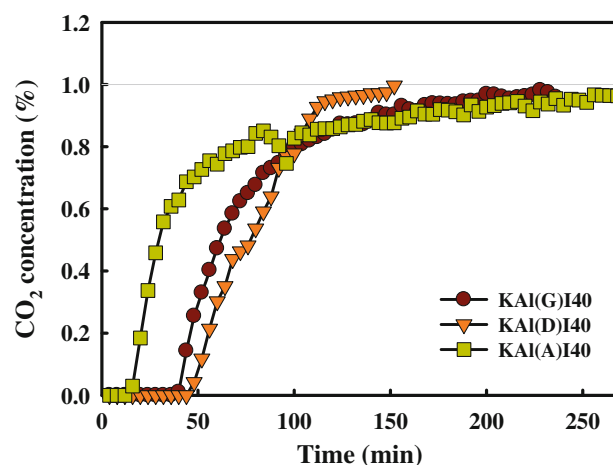


Fig. 8 Breakthrough curves of the KAl(G)I40, KAl(D)I40 and KAl(A)I40 sorbents at 1 cycle

per gram of K₂CO₃ in the KAl(A)I40 sorbent decreased. This was attributed to the limitation in increasing the amount of K₂CO₃ loaded in the potassium-based sorbent using α -Al₂O₃ as a support, because α -Al₂O₃ has a very small surface area. In a separate experiment, it was confirmed that the amount of K₂CO₃ loaded in the potassium-based sorbent was approximately 31.2 wt% by ICP-AES. On the other hand, the CO₂ capture capacity of the KAl(D)I40 sorbent was approximately 88 mg CO₂/g sorbent after two cycles. In particular, as shown in Fig. 8, both the breakthrough time of the KAl(D)I40 sorbent and the slope of a breakthrough curve after the breakthrough time were higher than those of the KAl(A)I40 sorbent. From these results, it was concluded that the KAl(D)I40 sorbent, which was prepared by the impregnation of δ -Al₂O₃ with 40 wt% K₂CO₃, can be used as a sorbent for post-combustion CO₂ capture owing to its high CO₂ capture and regeneration capacities, and excellent sorption rate.

4 Conclusions

This study examined the effects of the structure and textural properties of alumina on the CO₂ sorption and regeneration properties of the potassium-based alumina sorbents. The regeneration capacities of the KAl(B)I30, KAl(G)I30, KAl(G-A)I30, KAl(D)I30, KAl(A)I30, and KAl(A-A)I30 sorbents were 37.6, 46.5, 49.9, 74.3, 103.1 and 100.5 %, respectively. The deactivation problem of the alkali-based alumina sorbent using alumina can be solved using α -Al₂O₃ as a support. The regeneration capacity of the alkali-based alumina sorbent can be improved using δ -Al₂O₃ as a support. The results suggest that the regeneration capacities of the potassium-based alumina sorbents increased with increasing calcination temperature of alumina, even though

their CO₂ capture capacities were similar. The improved regeneration properties can be explained by the structural properties of alumina rather than by the effects of the textural properties. In particular, the KAl(D)I30 sorbent showed a high sorption rate compared to the other potassium-based alumina sorbents, even though the sorbent showed deactivation during multiple tests due to the formation of by-products. Based on these results, a new regenerable potassium-based δ -Al₂O₃ sorbent [KAl(D)I40], which was approximately 88 mg CO₂/g sorbent after 2 cycles, was developed for post-combustion CO₂ capture.

Acknowledgments This work was supported by R&D program under Agency for Defense Development, Republic of Korea. We acknowledge the financial support by grants from Korea CCS R&D Center, funded by the Ministry of Education, Science and Technology of Korean government. This work was supported by the Energy Efficiency & Resources of the Korea Institute of Energy Technology Evaluation and Planning (KETEP) grant funded by the Korea government Ministry of Knowledge Economy (2010201020007A).

References

- Abanades, J.C.: The maximum capture efficiency of CO₂ using a carbonation/calcination cycle of CaO/CaCO₃. *Chem. Eng. J.* **90**, 303–306 (2002)
- Arias, B., Grasa, G., Alonso, M., Abanades, J.C.: Post-combustion calcium looping process with a high stable sorbent activity by recarbonation. *Energy Environ. Sci.* **5**(6), 7353–7359 (2012)
- Chen, C., Yang, S.T., Ahn, W.S.: Calcium oxide as high temperature CO₂ sorbent: effect of textural properties. *Mater. Lett.* **75**, 140–142 (2012)
- Gupta, H., Fan, L.S.: Carbonation–calcination cycle using high reactivity calcium oxide for carbon dioxide separation from flue gas. *Ind. Eng. Chem. Res.* **41**, 4035–4042 (2002)
- Hagewiesche, D.P., Ashour, S.S., Al-Ghawas, H.A., Sandall, O.C.: Absorption of carbon dioxide into aqueous blends of monoethanolamine and N-methyldiethanolamine. *Chem. Eng. Sci.* **50**(7), 1071–1079 (1995)
- Hayashi, H., Taniuchi, J., Furuyashiki, N., Sugiyama, S., Hirano, S., Shigemoto, N., Nonaka, T.: Efficient recovery of carbon dioxide from flue gases of coal-fired power plants by cyclic fixed-bed operations over K₂CO₃-on-carbon. *Ind. Eng. Chem. Res.* **37**, 185–191 (1998)
- Hirano, S., Shigemoto, N., Yamaha, S., Hayashi, H.: Cyclic fixed-bed operations over K₂CO₃-on-carbon for the recovery of carbon dioxide under moist conditions. *Bull. Chem. Soc. Jpn.* **68**, 1030–1035 (1995)
- Intergovernmental Panel on Climate Change (IPCC): IPCC special report on carbon dioxide capture and storage. Cambridge University Press, Cambridge (2005)
- Kim, D.S., Han, S.J., Kwak, S.Y.: Synthesis and photocatalytic activity of mesoporous TiO₂ with the surface area, crystallite size, and pore size. *J. Colloid Interface Sci.* **316**, 85–91 (2007)
- Kwon, S.C., Fan, M., Dacosta, H.F.M., Russell, A.G., Tsouris, C.: Reaction kinetics of CO₂ carbonation with Mg-rich minerals. *J. Phys. Chem. A* **115**(26), 7638–7644 (2011)
- Lee, J.B., Ryu, C.K., Baek, J.I., Lee, J.H., Eom, T.H., Kim, S.H.: Sodium-based dry regenerable sorbent for carbon dioxide capture from power plant flue gas. *Ind. Eng. Chem. Res.* **47**, 4465–4472 (2008a)
- Lee, S.C., Choi, B.Y., Lee, T.J., Ryu, C.K., Ahn, Y.S., Kim, J.C.: CO₂ absorption and regeneration of alkali metal-based solid sorbents. *Catal. Today* **111**, 385–390 (2006)
- Lee, S.C., Kim, J.C.: Dry potassium-based sorbents for CO₂ capture. *Catal. Surv. Asia* **11**(4), 171–185 (2007)
- Lee, S.C., Chae, H.J., Lee, S.J., Choi, B.Y., Yi, C.K., Lee, J.B., Ryu, C.K., Kim, J.C.: Development of regenerable MgO-based sorbent promoted with K₂CO₃ for CO₂ capture at low temperatures. *Environ. Sci. Technol.* **42**(8), 2736–2741 (2008b)
- Lee, S.C., Chae, H.J., Park, Y.H., Ryu, C.K., Yi, C.K., Kim, J.C.: Novel regenerable potassium-based dry sorbents for CO₂ capture at low temperatures. *J. Mol. Catal. B Enzym.* **56**(2–3), 179–184 (2009)
- Lee, S.C., Kwon, Y.M., Ryu, C.Y., Chae, H.J., Ragupathy, D., Jung, S.Y., Lee, J.B., Ryu, C.K., Kim, J.C.: Development of new alumina-modified sorbents for CO₂ sorption and regeneration at temperatures below 200 °C. *Fuel* **90**, 1465–1470 (2011)
- Lee, S.C., Kwon, Y.M., Chae, H.J., Jung, S.Y., Lee, J.B., Ryu, C.K., Yi, C.K., Kim, J.C.: Improving regeneration properties of potassium-based alumina sorbents for carbon dioxide capture from flue gas. *Fuel* **104**, 882–885 (2013)
- Li, L., Wen, X., Fu, X., Wang, F., Zhao, N., Xiao, F., Wei, W., Sun, Y.: MgO/Al₂O₃ sorbent for CO₂ capture. *Energy Fuels* **24**, 5773–5780 (2010)
- Li, L., Li, Y., Wen, X., Wang, F., Zhao, N., Xiao, F., Wei, W., Sun, Y.: CO₂ capture over K₂CO₃/MgO/Al₂O₃ dry sorbent in a fluidized bed. *Energy Fuels* **25**, 3835–3842 (2011)
- Liang, Y., Harrison, D.P., Gupta, R.P., Green, D.A., McMichael, W.J.: Carbon dioxide capture using dry sodium-based sorbents. *Energy Fuels* **18**, 569–575 (2004)
- Mavroudi, M., Kaldis, S.P., Sakellariopoulos, G.P.: Reduction of CO₂ emissions by a membrane contacting process. *Fuel* **82**, 2153–2159 (2003)
- Okunev, A.G., Sharonov, V.E., Aistov, Y.I., Parmon, V.N.: Sorption of carbon dioxide from wet gases by K₂CO₃-in-porous matrix: influence of the matrix nature. *React. Kinet. Catal. Lett.* **71**(2), 355–362 (2000)
- Okunev, A.G., Sharonov, V.E., Gubar, A.V., Danilova, I.G., Paukshitis, E.A., Moroz, E.M., Kriger, T.A., Malakhov, V.V., Aistov, Y.I.: Sorption of carbon dioxide by the composite sorbent potassium carbonate in porous matrix. *Russ. Chem. Bull., Int. Ed.* **52**(2), 359–363 (2003)
- Salvador, C., Lu, D., Anthony, E.J., Abanades, J.C.: Enhancement of CaO for CO₂ capture in an FBC environment. *Chem. Eng. J.* **96**, 187–195 (2003)
- Seo, Y.W., Jo, S.H., Ryu, C.K., Yi, C.K.: Effects of water vapor pretreatment time and reaction temperature on CO₂ capture characteristics of a sodium-based solid sorbent in a bubbling fluidized-bed reactor. *Chemosphere* **69**, 712–718 (2007)
- Shigemoto, N., Yanagihara, T., Sugiyama, S., Hayashi, H.: Material balance and energy consumption for CO₂ recovery from moist flue gas employing K₂CO₃-on-activated carbon and its evaluation for practical adaptation. *Energy Fuels* **20**(2), 721–726 (2006)
- Siriwardane, R.V., Shen, M.S., Fisher, E.P., Poston, J.A.: Adsorption of CO₂ on molecular sieves and activated carbon. *Energy Fuels* **15**, 279–284 (2001)
- Stichert, W., Schuth, F.: Influence of crystallite size on the properties of zirconia. *Chem. Mater.* **10**, 2020–2026 (1998)
- Takamura, Y., Narita, S., Aoki, J., Hironaka, S., Uchida, S.: Evaluation of dual-bed pressure swing adsorption for CO₂ recovery from boiler exhaust gas. *Sep. Purif. Technol.* **24**, 519–528 (2001)
- Wilson, M., Tontiwachwuthikul, P., Chakma, A., Idem, R., Veawab, A., Aroonwilas, A., Gelowitz, D., Barrie, J., Mariz, C.: Test results from a CO₂ extraction pilot plant at boundary dam coal-fired power station. *Energy* **29**, 1259–1267 (2004)

- Yi, C.K., Jo, S.H., Seo, Y.W., Lee, J.B., Ryu, C.K.: Continuous operation of the potassium-based dry sorbent CO₂ capture process with two fluidized-bed reactors. *Int. J. Green Gas Cont.* **1**(1), 31–36 (2007)
- Yi, C.K., Jo, S.H., Seo, Y.W.: The effect of voidage on the CO₂ sorption capacity of K-based sorbent in a dual circulating fluidized bed process. *J. Chem. Eng. Jpn.* **41**(7), 691–694 (2008)
- Zhang, B.T., Fan, M., Bland, A.E.: CO₂ separation by a new solid K–Fe sorbent. *Energy Fuels* **25**, 1919–1925 (2011)
- Zhao, C.W., Chen, X.P., Zhao, C.S., Liu, Y.K.: Carbonation and hydration characteristics of dry potassium-based sorbents for CO₂ capture. *Energy Fuels* **23**(3), 1766–1769 (2009a)
- Zhao, C.W., Chen, X.P., Zhao, C.S.: CO₂ absorption using dry potassium-based sorbents with different supports. *Energy Fuels* **23**(9), 4683–4687 (2009b)
- Zhao, C.W., Chen, X.P., Zhao, C.S.: Effect of crystal structure on CO₂ capture characteristics of dry potassium-based sorbents. *Chemosphere* **75**, 1401–1404 (2009c)
- Zhao, C.W., Chen, X.P., Zhao, C.S.: K₂CO₃/Al₂O₃ for capturing CO₂ in flue gas from power plants. Part 4: abrasion characteristics of the K₂CO₃/Al₂O₃ sorbent. *Energy Fuels* **26**(2), 1395–1400 (2012)